



Published in final edited form as:

Nat Immunol. 2011 June ; 12(6): 527–535. doi:10.1038/ni.2036.

Genetic analysis of basophil function *in vivo*

Brandon M. Sullivan^{1,2,*}, Hong-Erh Liang^{1,2,*}, Jennifer K. Bando^{1,2}, Davina Wu^{1,2}, Laurence E. Cheng⁴, James K. McKerrow^{5,6}, Christopher D. C. Allen^{3,7}, and Richard M. Locksley^{1,2,3,7}

¹Howard Hughes Medical Institute, University of California San Francisco, San Francisco, CA, USA 94143

²Department of Medicine, University of California San Francisco, San Francisco, CA, USA 94143

³Department of Microbiology/Immunology, University of California San Francisco, San Francisco, CA, USA 94143

⁴Department of Pediatrics, University of California San Francisco, San Francisco, CA, USA 94143

⁵Department of Pathology, University of California San Francisco, San Francisco, CA, USA 94143

⁶Sandler Center for Basic Research in Parasitic Diseases, University of California San Francisco, San Francisco, CA, USA 94143

⁷Sandler Asthma Basic Research Center, University of California San Francisco, San Francisco, CA, USA 94143

Abstract

Contributions by basophils to allergic and helminth immunity remain incompletely defined. Using sensitive IL-4 reporter alleles, we demonstrate that basophil IL-4 production occurs by a CD4⁺ T cell-dependent process restricted to affected peripheral tissues. We genetically marked and specifically deleted basophils and demonstrate that basophils do not mediate T_H2 priming *in vivo*. Two-photon imaging confirmed that basophils do not interact with antigen-specific T cells in lymph nodes, but can engage in prolonged serial interactions with T cells in lung tissues. Although targeted deletion of IL-4 and IL-13 in either CD4⁺ T cells or basophils minimally impacted worm clearance, deletion from both lineages demonstrated a nonredundant role for basophil cytokines in primary helminth immunity.

Keywords

basophils; cytokines; T_H2 cells; allergic immunity; basophil reporter mice

INTRODUCTION

Helminth infections, affecting nearly 2.9 billion humans worldwide¹, elicit a stereotyped immune response with features shared by allergic and asthmatic reactions, including

Correspondence should be addressed to R. M. L. (locksley@medicine.ucsf.edu) or C. D. C. A. (chris.allen@ucsf.edu).

*These authors contributed equally.

The authors declare no competing financial interests.

Author Contributions

B.M.S., H-E.L., C.D.C.A., and R.M.L. conceived the work. H-E.L. generated Basoph8 reporter mice. B.M.S. designed and performed most experiments. C.D.C.A. contributed two-photon imaging data. J.K.B and B.M.S. performed analysis of basophils in the small intestine. D.W. and B.M.S generated data from mice infected with *S. mansoni* cercariae. L.E.C. analyzed mast cells in the skin in Basoph8 mice. J.K.M provided *S. mansoni* cercariae and eggs. B.M.S, C.D.C.A., and R.M.L. wrote the manuscript.

elevated serum IgE concentrations, excessive mucus production and tissue inflammation dominated by polarized T_H2 cells, eosinophils, mast cells and basophils. The linked cytokines IL-4 and IL-13, and their shared signaling components, the IL-4R α chain and STAT6, are required for allergic and anti-helminth immunity^{2, 3}. Although CD4⁺ T cells are required and T_H2 cells can produce these cytokines, innate sources of IL-4 and IL-13, such as basophils⁴ or lineage-negative IL-25- and IL-33-responsive cells⁵⁻⁷ – here designated innate type 2 helper cells, or iT_H2 cells, - can contribute to primary anti-helminth immunity. Immunohistochemical techniques are not adequate as yet to discern cytokine-producing cells *in situ*, and thus, a thorough assessment of their spatial and temporal relationships within tissues during the host response has been lacking.

Basophils are proposed to mediate B cell isotype switching and more recently, to drive CD4⁺ T helper cell differentiation⁸⁻¹⁰. Several studies have implicated basophils as antigen presenting cells that are necessary and sufficient for T_H2 priming¹¹⁻¹³, although this has been challenged by others¹⁴⁻¹⁷. Despite progress, the demonstration of basophil activation *in vivo* and a consensus understanding of their role in immunity are lacking, as recent attempts to mark these cells *in vivo* have not enabled unequivocal imaging of basophils in tissue^{16, 18}.

Here, we show that basophils are mobilized to multiple tissues during primary helminth infection, corroborating prior studies^{19, 20}, but that basophil IL-4 secretion is restricted to affected organs. We use a novel basophil reporter strain, termed Basoph8, to demonstrate that basophils are not required to initiate allergic immunity. Two-photon microscopy revealed that basophils do not interact with antigen-specific CD4⁺ T cells in inflamed lymph nodes, but can engage in serial interactions with CD4⁺ T cells in affected tissues, a process that correlated with sites of basophil activation. Basophil depletion did not affect clearance of *Nippostrongylus brasiliensis* in primary or secondary infections, but selective deletion of IL-4 and IL-13 from both basophils and CD4⁺ T cells revealed a non-redundant contribution of basophil-derived cytokines.

RESULTS

IL-4 production by basophils is restricted to involved tissues

We used mice with two independent markers targeted to the endogenous *Il4* locus in order to define which cells produce IL-4 during primary infection with *N. brasiliensis*²¹. These mice, designated KN2 \times 4get, are heterozygous for the 4get allele²², which expresses green fluorescent protein (GFP) from an internal ribosomal entry site (IRES) downstream of the IL-4 stop site, and the KN2 allele, which expresses human CD2 (hCD2) from the IL-4 start site and replaces the gene. When stimulated, cells from these mice reliably mark IL-4 competence by intracellular GFP expression and recent IL-4 protein secretion by the presence of membrane hCD2²¹. After infection, basophils, eosinophils and a fraction of CD4⁺ T cells comprised the major GFP⁺ cells recruited to the lungs²⁰, where they begin to accumulate by day 3. On day 5, basophils and CD4⁺ T cells began to express hCD2, consistent with IL-4 secretion *in vivo* (Fig. 1a). hCD2 expression was only observed in cells with enhanced GFP expression, thus providing an internal corroboration that activation of the 4get allele marks cells undergoing transcriptional activation of the IL-4 locus. The percentage of hCD2-positive basophils and CD4⁺ T cells peaked on days 5–6 in multiple experiments and then declined (Supplementary Fig. 1).

Previous reports using IL-4 reporter strains have described systemic basophil recruitment to tissues after *N. brasiliensis* infection^{19, 20}. While we also observed increased basophil numbers in many tissues, activation of basophil IL-4 secretion was tissue-restricted, since lung basophils expressed both GFP (IL-4 competence) and hCD2 (IL-4 secretion), whereas

basophils from spleen, liver, lymph node, blood and bone marrow (data not shown) expressed GFP, but not hCD2 (Fig. 1b and Supplementary Fig. 2). In contrast, CD4⁺ T cells that expressed both GFP and hCD2 were present in the spleen and lung, consistent with their ability to function as both cytokine-secreting follicular (T_{FH}; in spleen) and tissue effector (T_{H2}; in lung) T cells²³ (Fig. 1b and Supplementary Fig. 2). Basophils were also recruited to the small intestine (Supplementary Fig. 3). However, analysis of intestinal tissue was inconclusive between days 6–9 due to the substantial death of recovered cells, presumably a result of massive cellular activation, epithelial turnover and tissue injury. Eosinophils, despite their greater numbers and GFP-positive status, did not express large amounts of hCD2 (Fig. 1a). Using a YFP-marked IL-13 reporter strain of mice, we did not see IL-13 production by basophils (data not shown). As shown elsewhere, iH2 cells are readily marked as IL-13-producing cells after *N. brasiliensis* infection, but these cells, in contrast to basophils and CD4⁺ T cells, do not produce IL-4 *in vivo*⁷. Thus, basophils represent the early non-T cell source of IL-4 during helminth infection, in agreement with earlier studies^{19, 24}, and their activation *in vivo*, as illustrated using the KN2 × 4get reporter, is sequestered within affected tissues.

To define the requirements for basophil activation and the role of T_{H2} cells, we generated KN2 × 4get mice on the recombination activating gene (RAG)-2-deficient background. Compared to wild-type, lung tissues from these mice developed less inflammation with fewer basophils after infection, consistent with prior findings^{19, 20}, and recruited basophils did not express hCD2 (Fig. 1c). When reconstituted with *Il4*^{-/-} *Il13*^{-/-} CD4⁺ T cells, however, lungs were infiltrated with greater numbers of cells, including basophils that expressed hCD2 as a marker of recent IL-4 secretion (Fig. 1c). In multiple experiments, the infiltration and activation of basophils in the lungs of reconstituted mice was delayed by 1–2 days as compared to wild-type mice, either reflecting effects of T cell reconstitution or exposing an amplification role for T_{H2} cell-derived IL-4 and IL-13 *in vivo*. As expected, no serum IgE was detected in *Rag2*^{-/-} mice reconstituted with *Il4*^{-/-} *Il13*^{-/-} CD4⁺ T cells (data not shown).

We used an unrelated helminth model, infection with *Schistosoma mansoni*, to assess whether tissue-specific basophil activation could be visualized in the liver, which is a major site of the granulomatous response against trapped eggs²⁵. In contrast to basophils isolated from the liver in response to *N. brasiliensis*, basophils isolated from the livers of *S. mansoni*-infected KN2 × 4get *Rag2*^{-/-} mice that had been reconstituted with *Il4*^{-/-} *Il13*^{-/-} CD4⁺ T cells expressed hCD2, consistent with recent IL-4 secretion (Fig. 1d). Basophil activation in reconstituted mice was delayed compared to wild-type mice, likely reflecting as least in part the absence of IgE. As in primary *N. brasiliensis* infection, innate IL-4 protein expression was restricted to basophils, and liver eosinophils expressed little hCD2 (Fig. 1a,d). Thus, basophils are activated by a CD4⁺ T cell-dependent, but IL-4-, IL-13- and IgE-independent, mechanism in parasite-involved tissues.

CD4⁺ T cells mediate basophil IL-4 production by contact and IL-3

We sought to characterize the CD4⁺ T cell-derived factor(s) responsible for basophil activation in affected tissue. Although recruited to the spleen in relatively large numbers following *N. brasiliensis* infection, splenic basophils did not express hCD2 (Supplementary Fig. 2), perhaps reflecting an absence of interactions between spleen basophils and T cells during infection. To overcome potential restrictions *in vivo*, we isolated spleen cells from *N. brasiliensis*-infected KN2 × 4get mice and incubated them on plate-bound anti-CD3e overnight to promote T cell activation. When examined the next day, splenic basophils expressed hCD2, consistent with their activation to produce IL-4 (Fig. 2a). We next assessed whether basophil activation required direct contact with stimulated CD4⁺ T cells or could be provided by soluble, secreted factor(s) from activated CD4⁺ T cells. CD4⁺ T cells were

purified from the spleens of *N. brasiliensis*-infected mice (5–6 days post-infection) and basophils were enriched from the spleens of resting KN2 × 4get *Rag2*^{-/-} mice. To prevent cell-cell contact, a transwell insert was used to separate the purified CD4⁺ T cells and the basophils. As assessed by induction of hCD2, basophils were activated to produce IL-4 without CD4⁺ T cell contact (Fig. 2b), although to a lesser degree as compared to basophils in contact with activated T cells (Fig. 2a). Further, supernatants harvested after the overnight stimulation of CD4⁺ T cells from uninfected mice were sufficient to promote basophil hCD2 expression (Fig. 2c). IL-3 is implicated in promoting basophil expansion, survival and activation in the context of surface-bound IgE crosslinking^{26–28}. IL-3 was present in the stimulated CD4⁺ T cell supernatants (where it averaged 2.5 ng/ml) and IL-3 at these concentrations activated basophil IL-4 production *in vitro* (Fig. 2c). Additionally, neutralizing anti-IL-3 antibody inhibited basophil IL-4 production following incubation with the activated CD4⁺ T cell supernatant. However, IL-3 blockade did not block basophil activation when basophils were cultured together with CD4⁺ T cells (Fig. 2d). Consistent with our findings *in vivo*, CD4⁺ T cell-derived IL-4 and IL-13 and IgE were not required for basophil activation *in vitro*, as *Il4*^{-/-} *Il13*^{-/-} CD4⁺ T cells mediated basophil activation in the absence of antibodies (Fig. 2e). These data, as well as our findings in the context of *N. brasiliensis* infection, support a model in which basophil IL-4 production is restricted to involved tissues and dependent upon antigenic stimulation of CD4⁺ T cells by a process that optimally requires both direct contact with CD4⁺ T cells and IL-3.

Basoph8, a novel basophil reporter mouse strain

In order to track and delete basophils with high specificity, we replaced the mast cell protease-8 (*mcpt8*) gene at the start site by inserting a reporter cassette expressing YFP followed by an IRES and humanized Cre recombinase (hCre) (Fig. 3a and Supplementary Fig. 4). *Mcpt8* is a basophil gene in the conserved chymase locus, which has expanded in rodents through gene duplications to contain a number of species-specific genes^{29, 30}. *Mcpt8* is basophil-specific in mice and absent in humans, suggesting that it is not required for development of the basophil lineage. Prior reports targeting this locus have confirmed the specificity of gene expression in basophils^{16, 18}.

We analyzed tissues at the peak of the inflammatory response following *N. brasiliensis* infection and confirmed that all YFP-positive cells were basophils, characterized as SSC^{lo}, CD4⁻, c-Kit⁻, CD49b (DX5)⁺, βc (CD131), IL-3Rβ⁺, and IgE⁺ (Fig. 3b and data not shown). Further, isolation of basophils from Basoph8 mice by conventional flow cytometric analysis confirmed that all basophils from all tissues expressed YFP (Fig. 3d). The only discrepancy in YFP expression and conventional basophil markers occurred in the bone marrow, and was due to variegated expression of CD49b (DX5) within the Basoph8-positive population, likely highlighting developmental regulation of this adhesion molecule during basophil differentiation (Supplementary Fig. 5).

To delete basophils, we crossed Basoph8 mice with Rosa-DTα mice (Basoph8 × Rosa-DTα), which contain the diphtheria toxin-α gene inserted into the ubiquitous Rosa26 locus downstream of a loxp-flanked transcriptional stop site^{7, 31}. The Basoph8 × Rosa-DTα mice demonstrated highly efficient deletion of basophils, as assessed both by deletion of YFP⁺ cells and of basophils as identified using conventional staining (CD49b⁺, βc, IL-3Rβ⁺ SSC^{lo}) (Fig. 3c,d). Deletion was approximately 96% efficient after *N. brasiliensis* infection and surviving cells had noticeably attenuated YFP fluorescence (Fig. 3c,d). Mast cell numbers isolated after peritoneal lavage of *N. brasiliensis*-infected mice (Fig. 3e) and from the skin of older mice were unaffected, despite basophil deletion from blood and tissues (Fig. 3f and Supplementary Fig. 6). Eosinophils and CD4⁺ T cells likewise remained unaffected in Basoph8 × Rosa-DTα mice (see below).

Basophils are not required for priming CD4⁺ T cells *in vivo*

Recent studies suggest that basophils serve a necessary and sufficient role as antigen presenting cells (APC) in T_H2-associated immunity^{11–13}. Mechanistically, a model has been proposed in which basophils transiently migrate to draining lymph nodes, present peptide in the context of MHC class II and provide lineage-determining cytokines, all of which were necessary for efficient T_H2 priming. While APC function has been attributed to basophils, other work using different approaches has questioned a role for basophils in this process^{14–17}. To assess the requirement for basophils in T_H2-priming *in vivo*, we crossed basophil-deficient, Basoph8 × Rosa-DTα, mice onto the KN2 background. In this way, activation of IL-4 secretion from CD4⁺ T cells can be resolved by flow cytometry in the presence or absence of basophils without the need for restimulation of the cells *ex vivo*.

Immunization with *S. mansoni* eggs induced T_H2 priming in the draining lymph node within 3–4 days¹¹. Using established protocols, 2500 eggs were injected into the footpad of Basoph8 × KN2 and Basoph8 × Rosa-DTα × KN2 mice, and the accumulation of basophils and huCD2⁺ IL-4-secreting T cells was followed kinetically. Basophils were recruited to the draining popliteal lymph nodes following immunization, with a peak of approximately 3000–4000 cells at 48 h; basophils were virtually undetectable in Basoph8 × Rosa-DTα mice after similar challenge (Fig. 4a,b). Consistent with our observations in *N. brasiliensis*-infected mice, basophils did not express IL-4 in the draining lymph node at any time following *S. mansoni* immunization (Supplementary Fig. 7). Corroborating earlier studies¹¹, IL-4 secretion by lymph node CD4⁺ T cells as assessed by surface hCD2 expression was first detected at day 3 and peaked at day 4 (Fig. 4c,d). Over 99% of basophils were deleted in comparably challenged Basoph8 × Rosa-DTα × KN2 mice, but there was no decrease in the numbers of IL-4-secreting lymph node CD4⁺ T cells (Fig. 4c,d).

To test basophil requirements for allergic responses to soluble stimuli, similar groups of mice were challenged with the protease papain, which can induce a basophil influx into the draining lymph nodes followed 24 hours later by a T cell IL-4 response⁹. Using comparable conditions, however, the percentages and numbers of IL-4-producing CD4⁺ T cells were unaffected by the deletion of basophils in Basoph8 × Rosa-DTα × KN2 mice compared to basophil-replete Basoph8 × KN2 mice (Fig. 4e,f). Thus, using these novel reporter strains of mice, we could not demonstrate a basophil requirement for the CD4⁺ T cell responses to particulate or soluble IL-4-inducing stimuli.

Basophils interact with CD4⁺ T cells in effector tissue but not in lymph nodes

The data above indicated that basophils are dispensable for CD4⁺ T cell priming in lymph nodes, but that CD4⁺ T cells are essential for basophil activation in peripheral tissues, suggesting that the mode of interactions between basophils and CD4⁺ T cells differs between lymph nodes and peripheral tissues. To visualize these interactions, we took advantage of the Basoph8 mice, in which *mcpt8* drives high amounts of YFP fluorescence selectively in basophils. CD4⁺ T cells responding to immunization were visualized by the adoptive transfer of ovalbumin (OVA)-specific OT-II CD4⁺ T cells expressing DsRed or labeled with an orange dye. By modifying immunization models described above to include OVA, we could directly visualize the dynamics of the interactions between antigen-specific CD4⁺ T cells and basophils in time-lapse imaging by two-photon microscopy.

We observed robust expansion of OT-II cells and recruitment of basophils to the draining lymph node two days after subcutaneous immunization with *S. mansoni* eggs mixed with OVA. Between days 2 to 3, basophils occasionally contacted OT-II T cells, but these contacts were of very short duration and no stable conjugates were formed (Fig. 5a,b,c and Supplementary Video 1). Similar results were observed 2–3.5 days after subcutaneous

immunization with papain mixed with OVA (Supplementary Video 2). The lack of stable interactions between CD4⁺ T cells and basophils suggested that basophils do not act as APCs for CD4⁺ T cells in primary immune responses in lymph nodes.

For comparison, we visualized interactions between classical APCs and CD4⁺ T cells within lymph nodes. As reported in other systems³², we confirmed that prolonged CD4⁺ T cell interactions with dendritic cells could be observed within the first day after papain immunization, but these interactions subsided by days 2–3 when basophils were recruited (data not shown). As T cell-B cell interactions typically occur during this time³³, we co-transferred OT-II T cells and CFP-expressing Hy10 B cells, specific for avian egg lysozyme, into Basoph8 recipients. After subcutaneous immunization with papain mixed with a conjugate of duck egg lysozyme and OVA (DEL-OVA), we could observe basophils, OT-II T cells and Hy10 B cells together in the imaging field. Interactions between OT-II T cells and Hy10 B cells were much longer than OT-II T cells with basophils, and a number of stable conjugates between OT-II T cells and Hy10 B cells could be observed, some of which exceeded the duration of the recording (Fig. 5a,b,c and Supplementary Video 3). These prolonged T cell-B cell interactions were comparable to those that occur in mice immunized with DEL-OVA mixed with a classical adjuvant monophosphoryl lipid A (MPL) and trehalose dicorynomycolate (TDM) (data not shown). Thus, at the time in which basophils are recruited to the lymph node, CD4⁺ T cells are engaged in prolonged interactions with B cells in a manner independent of basophil interactions.

To visualize the interaction dynamics of OT-II T cells and basophils in the lungs, we infected mice with *N. brasiliensis* and then administered intranasal OVA. In explanted lung slices, we found basophils and OT-II T cells together in small regions of the lung near hemorrhagic sites where *N. brasiliensis* larvae had penetrated the blood vessels. We observed interactions between OT-II T cells and basophils in the lung that were significantly longer than the brief contacts in lymph nodes (Fig. 5a,b,c and Supplementary Video 4). To confirm that basophils could also interact with non-transgenic T cells, we imaged Basoph8 mice expressing a human CD2-DsRed transgene that illuminated the entirety of polyclonal T cells and observed very similar interactions in the lungs after *N. brasiliensis* infection (Supplementary Video 5).

Unexpectedly, in several instances in both systems we observed that an individual T cell and basophil in the lung would come in contact with each other for a few minutes, disengage, and then come back in contact, in a repetitive fashion (Fig. 5a and Supplementary Videos 4 and 5). Unlike the stable T-B conjugates observed in lymph nodes in which the T cells closely track the B cell movements³⁴, the T cells and basophils in the lungs did not closely follow each other's movements (Supplementary Fig. 8). Instead, the T cells and basophils would alternately pull away from each other and move toward each other even while remaining in contact. This distinction was further reflected by quantifying the distance between the centroids (center of mass) of the cells (Fig. 5d,e). The median distances between centroids of T cells and basophils were significantly longer than that for T cells and B cells while the cells were in contact. Taken together, these data indicate that CD4⁺ T cells and basophils engage in multiple serial interactions in affected lung of short to moderate duration, in contrast to the very brief contacts observed in lymph nodes, but also in a manner distinct from the close stable conjugates formed between T cells and B cells.

Basophil-derived cytokines contribute to worm clearance

Prior studies have suggested modest contributions by basophils in the host response to *N. brasiliensis*¹⁶. Using Basoph8 and Basoph8 × Rosa-DTα mice, we could demonstrate no effect of basophil deletion on worm clearance, total lung cellularity, numbers of infiltrating CD4⁺ T cells or eosinophils, or serum IgE concentration during primary infection (Fig.

6a,b,c). Secondary infection of mice with *N. brasiliensis* results in a greatly accelerated response and the few worms that reach the intestine are expelled within 5 days. Using KN2 × 4get mice to assess the secondary response, we observed greater numbers of IL-4-producing basophils in the lung at earlier time points (Supplementary Fig. 9a). In contrast to the primary response, the accelerated secondary response was almost entirely due to IL-4-dependent-IgE because mice reconstituted with *Il4*^{-/-} *Il13*^{-/-} CD4⁺ T cells, which lack IgE and high-affinity IgG1, did not manifest this augmented basophil cytokine response despite the development of tissue inflammation and basophilia (Supplementary Fig. 9a,b). Indeed, when serum was harvested from *N. brasiliensis*-infected wild-type or *Rag2*^{-/-} mice and adoptively transferred to KN2 × 4get *Rag2*^{-/-} mice that had been reconstituted with *Il4*^{-/-} *Il13*^{-/-} CD4⁺ T cells, the augmented basophil cytokine response was dependent on reconstitution by wild-type, but not *Rag2*^{-/-}-serum. In contrast to *Rag2*^{-/-} serum, wild-type serum resulted in decoration of the basophil surface with IgE (Supplementary Fig. 9c). In contrast to findings with another basophil-deficient strain¹⁶, we observed no deficits in worm clearance or tissue eosinophil infiltration by basophil-deficient Basoph8 × Rosa-DTα mice during secondary infection with *N. brasiliensis* (Supplementary Fig. 10).

Although we could discern no requirement for basophils as assessed by their deletion, the activation of IL-4 secretion by basophils in tissues raised the possibility that cytokines produced by these cells are redundant within the context of infection. Since both T_H2 cells and basophils secrete cytokines in affected tissues (Fig. 1a,b), we generated mice with loxP sites engineered into the *Il4* and *Il13* locus such that Cre-mediated recombination would result in deletion of both genes³⁵. The homozygous mice, designated *Il4-Il13*^{fl/fl}, were crossed to *Il4*^{-/-} *Il13*^{-/-}, CD4-cre and Basoph8 mice to facilitate lineage-specific deletion of the cytokines from CD4⁺ T cells (*Cd4-cre* × *Il4-Il13*^{fl/-}) from basophils (Basoph8 × *Il4-Il13*^{fl/-}), or from both cells (*Cd4-cre* × Basoph8 × *Il4-Il13*^{fl/-}) in order to assess their contributions to the host cytokine response. Deletion of IL-4 and IL-13 from CD4⁺ T cells did not greatly impact the capacity to expel worms during primary infection despite the absence of IgE (Fig. 6d,e). Deletion of IL-4 and IL-13 from basophils also did not impact worm clearance, but conversely had no effect on serum IgE concentrations (data not shown). In contrast, simultaneous deletion of IL-4 and IL-13 from both CD4⁺ T cells and basophils resulted in a significant increase in the intestinal worm burden (Fig. 6d,e), indicating that cytokines from both of these lineages contribute to the host response against migratory helminthes.

DISCUSSION

Although described by Paul Ehrlich in 1879 and conserved in all vertebrates, including fish, birds and reptiles, basophils remain enigmatic and a precise delineation of their role has remained elusive due to the lack of adequate reagents to address their specific contributions³⁶. Seminal studies in the 1990's first identified a non-B, non-T cell as a major source of IL-4 after parasite challenge that was revealed after FcεRI cross-linking and augmented by IL-3³⁷⁻⁴⁰. Subsequently, two different IL-4 reporter mice were used to demonstrate that basophils accumulate in tissues through a CD4⁺ T cell-dependent but STAT6-independent mechanism^{19, 20}. Attempts to deplete basophils using various antibodies^{11, 12, 17, 41-43} have resulted in controversy regarding the sensitivity and specificity of the targeted deletion¹⁵, and two groups subsequently targeted the basophil-specific *mcpt8* gene to achieve lineage marking^{16, 18}. Here, we combine novel IL-4 reporter mice with newly generated mcpt8 basophil reporter mice, designated Basoph8, that uses a different targeting strategy that allows direct visualization of basophils in living tissues as well as generation of basophil-deficient mice. Using these mice, we report several findings, including the CD4⁺ T cell-dependent localization of basophil IL-4 production to tissues involved by parasites; replication of the CD4⁺ T cell-dependent ability to activate IL-4

production from basophils *in vitro* through a contact- and IL-3-dependent but IgE-independent process; and evaluation of basophil dynamics *in vivo* that corroborates basophil interactions with antigen-specific CD4⁺ T cells in tissues, but not in draining lymph nodes. Finally, using lineage-specific deletion of the *Il4* and *Il13* genes from CD4⁺ T cells and basophils, we reveal cooperativity between these cells in the primary response to migratory helminthes.

The signals from CD4⁺ T cells that recruit and license basophils to secrete IL-4 during the primary response are of much interest. IL-3 is an important basophil differentiation and growth factor, capable of expanding basophils from bone marrow *in vitro* and *in vivo*. IL-3 from activated CD4⁺ T cells was important in mobilizing basophils from the bone marrow during infection with *N. brasiliensis*, as *Rag2*^{-/-} mice reconstituted with IL-3-deficient CD4⁺ T cells had reduced numbers of bone marrow and blood basophils as compared to mice reconstituted with wild-type T cells²⁸. Additionally, IL-3 mediated basophil recruitment to lymph nodes following helminth infection⁴⁴. As shown here, recombinant IL-3 or IL-3 accumulating in supernatants of activated CD4⁺ T cells stimulated IL-4 production from basophils *in vitro*. However, maximal IL-4 production occurred when basophils were co-cultured with activated CD4⁺ T cells, suggesting that direct cell contact likely contributes additional signals. Indeed, neutralizing IL-3 antibodies did not block basophil IL-4 production *in vitro*, and optical imaging studies of live tissues demonstrated CD4⁺ T cell and basophil interactions in lung, but not lymph nodes, which support a contact-driven requirement for tissue basophil activation. More work will be required to examine the parameters of this process, but the tools we have generated will now facilitate further study.

An intriguing aspect of basophil biology has been the recent reports in various systems that invoke a role for basophils as primary APCs in T_H2-dominated immunity¹¹⁻¹³. These studies used non-specific monoclonal antibodies to achieve basophil depletion and subsequent studies have raised questions regarding the specificity of the antibodies such that off-target deletion of other critical immune cells, such as dendritic cells, may have occurred^{14, 15, 17}. Clearly, lineage tracking of basophils is needed to investigate this process, and two groups have reported targeting the *mcpt8* locus in mice as we report here^{16, 18}. Mcpt8 is a basophil-specific protease in mice whose enzymatic substrate remains unknown^{29, 45}. In the first reporter strain, designated Mcpt8^{DTR}, a downstream IRES was followed by a diphtheria toxin receptor-enhanced GFP fusion protein that enabled diphtheria-mediated depletion of basophils that was sustained up to 5 days after injection of toxin¹⁸. These mice were used to demonstrate a requirement for basophils to impede tick re-feeding on mice by a process dependent on antibody and basophil Fc receptors¹⁸. In the second reported strain, BAC-transgenic mice were generated with Cre recombinase replacing the *mcpt8* gene, which resulted in unexpected constitutive deletion of approximately 90% of basophils by a process believed to be mediated by Cre-dependent toxicity from the 5- to 7-copy integration events¹⁶. These mice were used to demonstrate no requirements for basophils in various allergic immune models, including papain- and OVA-induced allergy models, while supporting a role for basophils in IgE-mediated chronic dermatitis, confirming earlier studies^{16, 46}. Additionally, a role for basophils was suggested in secondary, but not primary, *N. brasiliensis* infection, as eosinophil and T_H2 cell recruitment to the lung and worm clearance were diminished¹⁶.

In the Basoph8 mice we report, the *mcpt8* gene was replaced by YFP-IRES-Cre that established bright YFP fluorescence in basophils and enabled conditional deletion of the cells or their cytokines. Studies with these mice enabled us to assess the positioning of basophils in tissues, their relationships with CD4⁺ T cells on which they depend for functional activity and the consequence of specific basophil-restricted deletion of IL-4 and

IL-13 to assess directly the contributions of these cytokines from basophils. Regarding basophil entry into inflamed lymph nodes, we confirm basophil entry with soluble (papain) and particulate stimuli (schistosome eggs), but can show no requirement for basophils for activation of IL-4 production by naïve CD4⁺ T cells as assessed in the deleter strain. This observation was corroborated independently by flow cytometry using cells from mice with sensitive IL-4 reporter alleles to demonstrate that basophils do not produce IL-4 in lymphoid tissues. Additionally, we present imaging studies to show that basophils do not interact with CD4⁺ T cells in a manner consistent with their proposed role as APCs. Finally, we specifically remove IL-4 and IL-13 from basophils and confirm that these cytokines do not contribute to host IgE or immunity to *N. brasiliensis* when CD4⁺ T cells are intact. We conclude through these multiple corroborating yet independent lines of investigation that basophils are not required to initiate primary cellular or humoral immunity under the conditions examined.

Prior studies have implicated CD4⁺ T cells as necessary for basophil accumulation^{19, 20}. Using these novel mouse reagents, we demonstrate that the CD4⁺ T cell requirement is necessary to mediate basophil IL-4 secretion, which is sequestered to tissues involved by parasites and infiltrated by activated CD4⁺ T cells. Although IL-4 and IL-13 from neither CD4⁺ T cells nor basophils were alone required to expel intestinal *N. brasiliensis* after primary infection, combined deletion of IL-4 and IL-13 from both cell types resulted in a significant and reproducible deficit in this response, revealing a contribution by basophil-derived IL-4 to this process. IgE responses were completely dependent on CD4⁺ T cell-derived IL-4 and IL-13. In contrast to an earlier study¹⁶, we could demonstrate no deficit in immunity to secondary *N. brasiliensis* infections using basophil-deficient mice. Under conditions examined here, augmented basophil IL-4 production in secondary infection was entirely immunoglobulin-dependent, as demonstrated by serum adoptive transfer. As such, our data are most consistent with models of tick infestation and chronic allergic dermatitis in uncovering interacting roles for basophils and immunoglobulin^{16, 18}. Thus, basophils, despite their identification as innate immune cells, are peculiarly dependent on adaptive immune cells, including CD4⁺ T cells and antibodies, for robust generation of IL-4 in these model systems.

Although combined deletion of IL-4 and IL-13 from CD4⁺ T cells and basophils reproducibly impaired intestinal worm clearance, the numbers of intestinal worms were consistently fewer than in infected *Rag2*^{-/-} or in *Il4*^{-/-} *Il13*^{-/-} mice^{47, 48}. Recently, contributions of other cells, variably referred to as natural helper cells, nuocytes and iH2 cells, have been revealed⁵⁻⁷. These cells produce high concentrations of IL-13 and IL-5, but, like basophils, require CD4⁺ T cells for optimal activity⁵. We speculate that iH2 cells are responsible for the partial worm clearance in the setting of CD4⁺ T cell and basophil IL-4 and IL-13-deficiency, although it is important to note the overlapping effects of IL-4, IL-13, IL-5 and IL-9 as assessed by stepwise deletion of these genes while assessing effects on worm immunity⁴⁹. Basoph8 mice will provide a novel reagent to explore the role of basophils in infectious and inflammatory models in addition to the ones explored here, and to place these cells within the context of additional cell types and cytokines implicated in allergic immunity and the response to helminthes.

ONLINE METHODS

Mice

KN2 × 4get, IL-4 dual reporter mice have been described²¹. KN2 and 4get mice were bred individually to the *Rag2*^{-/-} background and intercrossed to derive KN2 × 4get *Rag2*^{-/-} on the BALB/c background. *Il4-Il13*^{f1/f1} and Rosa-DTα mice have been described^{31, 35}. *Cd4-cre* mice and OT-II.2 (subline 425-2) mice on a *Rag1*^{-/-} C57BL/6 background were purchased

from Taconic. Hemizygous OT-II.2 (subline 426-6) mice⁵⁰ were repeatedly bred to human CD2-DsRed transgenic mice⁵¹ until the fluorescent reporter was homozygous. Hy10 (formerly VDJ9/k5) mice⁵² were bred to β -actin-CFP mice (The Jackson Laboratory #004218; Tg(ACTB-ECFP)1Nagy/J). Imaging of T cell interactions with DCs was by adoptive transfer of OT-II T cells into CD11c-YFP transgenic mice, C57BL/6 background⁵³. Mice were maintained in specific pathogen-free facilities at UCSF according to institutional guidelines.

Generation of Basoph8 mice

A composite fluorescent reporter/recombinase cassette was assembled by standard cloning procedures in the following order: rabbit β -globin gene partial exon 2–3 genomic sequence serves as an artificial intron and splicing donor/acceptor; EYFP (Clontech) gene as fluorescent reporter; encephalomyocarditis virus (EMCV) internal ribosome entry site (IRES); P1 phage Cre-recombinase cDNA with codon usage optimized for mammalian cells (hCre); bovine growth hormone (bGH) poly-adenylation signal (pA); a floxed-neomycin-resistant cassette derived from pL2neo2 placed 3' of the entire cassette. This 4.8 kb reporter/recombinase cassette was cloned into a basal targeting construct pKO915-DT (Lexicon) containing diphtheria toxin- α chain (DT) for negative selection. 5' and 3' homologous arms used to flank the reporter/recombinase cassette were obtained by high-fidelity PCR amplification of the *mcpt8* locus from 129/SvJ genomic DNA. The 5' arm consists of a 2.9 kb fragment covering the promoter region and 5' UTR. The 3' arm consists of a 2.6 kb fragment spanning the endogenous start codon to exon 5 of the *mcpt8* gene. The NotI-linearized construct was electroporated into PrmCre ES cells, which express Cre recombinase driven by the protamine promoter. G418-resistant ES clones were screened for homologous recombination by Southern blot. Two independent clones were injected into C57BL/6 blastocysts to generate chimeras. The neomycin-resistant cassette was deleted in the male germline by Cre-mediated recombination after breeding male chimeras to wild-type C57BL/6 females. Mice carrying the Basoph8 allele were backcrossed to either the C57BL/6 or BALB/c background.

Parasites and papain immunization

The maintenance and infection with *N. brasiliensis* have been described²⁰. *S. mansoni* were maintained as described, and mice were infected with 200 or 260 cercariae by subcutaneous injection⁵⁴. Liver samples were processed for flow cytometry analysis or fixed in 4% paraformaldehyde for histology. *S. mansoni* eggs were harvested from hamster livers and 2500 eggs were injected subcutaneously in 50 μ l into the footpad of mice as described¹¹. Mice were immunized with 50 μ g papain (Calbiochem) as described⁹. For lymph node imaging experiments, *S. mansoni* eggs or papain were mixed with 0.5–1 mg/mL OVA (albumin from chicken egg white, grade VII, Sigma-Aldrich) or 0.1–0.33 mg/mL DEL-OVA⁵². Mice were immunized subcutaneously on both lower flanks and bilaterally proximal to the base of the tail with 25 μ L per site. This subcutaneous immunization resulted in basophil recruitment to the draining inguinal lymph nodes that was comparable to the popliteal lymph node after footpad immunization (data not shown). In control experiments, an equivalent dose of DEL-OVA was mixed with Sigma Adjuvant System containing MPL and TDM (Sigma-Aldrich). To activate OT-II T cells in the lungs after *N. brasiliensis* infection, mice were lightly anesthetized with isoflurane and 50 μ g of OVA was given intranasally in 50 μ l of PBS on days 1 and 6 after infection.

Flow cytometry

Antibodies against CD4 (APC-Alexa780), CD131/ β c (PE), c-Kit (APC, biotinylated), and CD44 (APC) were purchased from Pharmingen; DX5 (APC) and c-Kit (APC-eFluor780) from eBioscience; human CD2 (hCD2) (PE) and mouse IgG2a (PE) from Invitrogen. Cells

were incubated with anti-CD16/32 (Pharmingen), stained with the appropriate antibodies and labeled with the vital dye 4',6-diamidino-2-phenylindole (DAPI), 1 $\mu\text{g/ml}$, (Roche). Cell counts were determined using Caltag Counting Beads (Invitrogen). The gating strategy used for hCD2 staining is provided (Supplementary Fig. 11). The frequency of HEL-binding B cells was determined by flow cytometry as described⁵². The frequency of TCR-transgenic T cells was determined by flow cytometry⁵² with the following antibodies: rat anti-mouse V α 2 TCR (clone B20.1, PerCP-Cy5.5, Biolegend), mouse anti-mouse V β 5.1,5.2 TCR (clone MR9-4, FITC, BD Biosciences), rat anti-mouse CD4 (clone GK1.5, APC-H7, BD Biosciences) and hamster anti-mouse CD3 (clone 145-2C11, Alexa 647, Biolegend) or rat anti-mouse CD3 (clone 17A2, Pacific Blue, Biolegend). Cells were analyzed on an LSRII (Becton Dickinson) and data were analyzed using FlowJo software (Treestar, Inc.).

Cell purification, labeling, and adoptive transfers

For CD4⁺ T cell reconstitution of KN2 \times 4get *Rag2*^{-/-} mice, axillary, brachial, cervical, inguinal, popliteal and mesenteric lymph nodes were isolated from *Il4*^{-/-} *Il13*^{-/-} mice. CD4⁺ T cells were purified from single-cell suspensions by negative depletion using antibody-coated magnetic bead isolation (Miltenyi Biotec), and 1×10^7 cells were transferred to KN2 \times 4get *Rag2*^{-/-} mice by tail vein injection. Animals were infected with *N. brasiliensis* 1 week later.

Details of cell purification and labeling for the imaging experiments are described in the Supplementary Methods. Briefly, B cells were purified by CD43 and CD11c negative selection. CD4 T cells were purified with the Dynabeads FlowComp Mouse CD4 kit (Invitrogen). In some cases in which small numbers of cells were being transferred (<25,000 T cells or <50,000 B cells per recipient), no purification was needed and approximately 250 μL of blood was collected from the retro-orbital plexus of anesthetized donor mice with heparinized capillary tubes (Fisher Scientific) into microtainer tubes with EDTA (BD). Erythrocytes were lysed with ACK Lysing Buffer (Quality Biological) and cells were resuspended in PBS. Cells were adoptively transferred into the retro-orbital plexus of anesthetized Basoph8 mice 12–24 hours prior to immunization.

In vitro basophil activation

Total splenocytes from day 5–6 *N. brasiliensis*-infected KN2 \times 4get mice were stimulated, using 1×10^6 CD4⁺ T cells/ml, overnight on plate-bound anti-mouse CD3 ϵ (2 $\mu\text{g/ml}$) (clone 145-2C11) (BD Pharmingen). Splenic CD4⁺ T cells were isolated from *N. brasiliensis*-infected mice by positive magnetic bead selection (L3T4, Miltenyi Biotec) and incubated overnight at $2 \times 10^6/\text{ml}$ on plate-bound anti-mouse CD3 ϵ . Supernatants were collected and analyzed for cytokines by ELISA. Basophils were enriched from the spleens of KN2 \times 4get *Rag2*^{-/-} mice using negative bead selection of CD49b-positive cells (Miltenyi Biotec). Enriched basophils, $40\text{--}60 \times 10^4$, were stimulated overnight in 1 ml of activated-CD4⁺ T cell supernatant or recombinant IL-3 (R&D Systems), and basophil hCD2 expression was assessed by flow cytometry as described.

Two-photon microscopy and data analysis

Details of the lung slice and lymph node explant preparation and imaging setup are described in the Supplementary Methods. Briefly, lung slices were prepared for imaging by a modification of established methods (E. Thornton and M. Krummel, manuscript in preparation)⁵⁵. The lungs were inflated with agarose, which was allowed to solidify, and then thick slices were cut on a vibratome. Lung slices and explanted lymph nodes were perfused in an imaging chamber with warmed RPMI media bubbled with 95% O₂ and 5% CO₂ and the temperature was maintained at 35–37°C.

Two-photon microscopy was on an upright LSM 7 MP (Carl Zeiss MicroImaging), outfitted with a W Plan-Apochromat 20x/1.0 N.A. water-immersion objective, acousto-optical modulator, motorized stage (Prior Scientific), Chameleon Ultra II laser (Coherent), and ZEN 2009 software. Each *xy* plane was collected at a resolution of 512×512 pixels with bidirectional scanning and variable zoom. The spacing between planes in the *z* dimension was set to 3–5 times the *xy* pixel size for a given zoom setting. Both Basoph8 YFP fluorescence and CFP were detected in a sensitive gallium arsenide phosphide (GaAsP) detector and were spectrally separated by changing the laser excitation wavelength (for details, see Supplementary Methods). DsRed or CMTMR were collected on a standard non-descanned detector (NDD) through an ET605/70 emission filter (Chroma).

Contact times were determined by a semi-automated measurement task in Volocity 5.2.1 or 5.4.2 (PerkinElmer) and data were analyzed with Microsoft Excel 2003 and GraphPad Prism. Details are provided in the Supplementary Methods. Maximum intensity *z*-projection still images and time-lapse sequences were prepared in Metamorph 7.7 (Molecular Devices) and ZEN 2009 Light Edition (Carl Zeiss MicroImaging), respectively. Linear adjustments were made to brightness and contrast and in some cases photobleaching was partially corrected by interpolation. Images were processed with low pass or median noise filters. Annotation and final compilation of videos was in Adobe After Effects 7.0. QuickTime format videos were compressed with a JPEG-2000 codec.

Supplementary Material

Refer to Web version on PubMed Central for supplementary material.

Acknowledgments

We thank K.C. Lim and N. Flores for technical support, and E. Thornton and M. Krummel for training in lung slice preparation. D. Kioussis kindly provided huCD2-DsRed transgenic mice. J. Cyster provided mice and use of his two-photon microscope. This work was supported by the NIH AI026918 and AI077439, the HHMI, and the Sandler Asthma Basic Research Center at UCSF.

References

1. Chan MS. The global burden of intestinal nematode infections--fifty years on. *Parasitol Today*. 1997; 13:438–443. [PubMed: 15275146]
2. Urban JF Jr, Maliszewski CR, Madden KB, Katona IM, Finkelman FD. IL-4 treatment can cure established gastrointestinal nematode infections in immunocompetent and immunodeficient mice. *J Immunol*. 1995; 154:4675–4684. [PubMed: 7722320]
3. Urban JF Jr, et al. IL-13, IL-4Ralpha, and Stat6 are required for the expulsion of the gastrointestinal nematode parasite *Nippostrongylus brasiliensis*. *Immunity*. 1998; 8:255–264. [PubMed: 9492006]
4. Voehringer D, Reese TA, Huang X, Shinkai K, Locksley RM. Type 2 immunity is controlled by IL-4/IL-13 expression in hematopoietic non-eosinophil cells of the innate immune system. *J Exp Med*. 2006; 203:1435–1446. [PubMed: 16702603]
5. Neill DR, et al. Nuocytes represent a new innate effector leukocyte that mediates type-2 immunity. *Nature*. 2010; 464:1367–1370. [PubMed: 20200518]
6. Moro K, et al. Innate production of T(H)2 cytokines by adipose tissue-associated c-Kit(+)/Sca-1(+) lymphoid cells. *Nature*. 2010; 463:540–544. [PubMed: 20023630]
7. Price AE, et al. Systemically dispersed innate IL-13-expressing cells in type 2 immunity. *Proc Natl Acad Sci U S A*. 2010; 107:11489–11494. [PubMed: 20534524]
8. Oh K, Shen T, Le Gros G, Min B. Induction of Th2 type immunity in a mouse system reveals a novel immunoregulatory role of basophils. *Blood*. 2007; 109:2921–2927. [PubMed: 17132717]
9. Sokol CL, Barton GM, Farr AG, Medzhitov R. A mechanism for the initiation of allergen-induced T helper type 2 responses. *Nat Immunol*. 2008; 9:310–318. [PubMed: 18300366]

10. Yanagihara Y, et al. Cultured basophils but not cultured mast cells induce human IgE synthesis in B cells after immunologic stimulation. *Clin Exp Immunol.* 1998; 111:136–143. [PubMed: 9472673]
11. Perrigoue JG, et al. MHC class II-dependent basophil-CD4+ T cell interactions promote T(H)2 cytokine-dependent immunity. *Nat Immunol.* 2009; 10:697–705. [PubMed: 19465906]
12. Sokol CL, et al. Basophils function as antigen-presenting cells for an allergen-induced T helper type 2 response. *Nat Immunol.* 2009; 10:713–720. [PubMed: 19465907]
13. Yoshimoto T, et al. Basophils contribute to T(H)2-IgE responses in vivo via IL-4 production and presentation of peptide-MHC class II complexes to CD4+ T cells. *Nat Immunol.* 2009; 10:706–712. [PubMed: 19465908]
14. Phythian-Adams AT, et al. CD11c depletion severely disrupts Th2 induction and development in vivo. *J Exp Med.* 2010; 207:2089–2096. [PubMed: 20819926]
15. Hammad H, et al. Inflammatory dendritic cells—not basophils—are necessary and sufficient for induction of Th2 immunity to inhaled house dust mite allergen. *J Exp Med.* 2010; 207:2097–2111. [PubMed: 20819925]
16. Ohnmacht C, et al. Basophils orchestrate chronic allergic dermatitis and protective immunity against helminths. *Immunity.* 2010; 33:364–374. [PubMed: 20817571]
17. Tang H, et al. The T helper type 2 response to cysteine proteases requires dendritic cell-basophil cooperation via ROS-mediated signaling. *Nat Immunol.* 2010; 11:608–617. [PubMed: 20495560]
18. Wada T, et al. Selective ablation of basophils in mice reveals their nonredundant role in acquired immunity against ticks. *J Clin Invest.* 2010; 120:2867–2875. [PubMed: 20664169]
19. Min B, et al. Basophils produce IL-4 and accumulate in tissues after infection with a Th2-inducing parasite. *J Exp Med.* 2004; 200:507–517. [PubMed: 15314076]
20. Voehringer D, Shinkai K, Locksley RM. Type 2 immunity reflects orchestrated recruitment of cells committed to IL-4 production. *Immunity.* 2004; 20:267–277. [PubMed: 15030771]
21. Mohrs K, Wakil AE, Killeen N, Locksley RM, Mohrs M. A two-step process for cytokine production revealed by IL-4 dual-reporter mice. *Immunity.* 2005; 23:419–429. [PubMed: 16226507]
22. Mohrs M, Shinkai K, Mohrs K, Locksley RM. Analysis of type 2 immunity in vivo with a bicistronic IL-4 reporter. *Immunity.* 2001; 15:303–311. [PubMed: 11520464]
23. Reinhardt RL, Liang HE, Locksley RM. Cytokine-secreting follicular T cells shape the antibody repertoire. *Nat Immunol.* 2009; 10:385–393. [PubMed: 19252490]
24. van Panhuys N, et al. Basophils Are the Major Producers of IL-4 during Primary Helminth Infection. *J Immunol.* 2011
25. Pearce EJ, MacDonald AS. The immunobiology of schistosomiasis. *Nat Rev Immunol.* 2002; 2:499–511. [PubMed: 12094224]
26. Lantz CS, et al. Role for interleukin-3 in mast-cell and basophil development and in immunity to parasites. *Nature.* 1998; 392:90–93. [PubMed: 9510253]
27. Lantz CS, et al. IL-3 is required for increases in blood basophils in nematode infection in mice and can enhance IgE-dependent IL-4 production by basophils in vitro. *Lab Invest.* 2008; 88:1134–1142. [PubMed: 18975389]
28. Shen T, et al. T cell-derived IL-3 plays key role in parasite infection-induced basophil production but is dispensable for in vivo basophil survival. *Int Immunol.* 2008
29. Poorafshar M, Helmbly H, Troye-Blomberg M, Hellman L. MMCP-8, the first lineage-specific differentiation marker for mouse basophils. Elevated numbers of potent IL-4-producing and MMCP-8-positive cells in spleens of malaria-infected mice. *Eur J Immunol.* 2000; 30:2660–2668. [PubMed: 11009100]
30. Gallwitz M, Hellman L. Rapid lineage-specific diversification of the mast cell chymase locus during mammalian evolution. *Immunogenetics.* 2006; 58:641–654. [PubMed: 16807746]
31. Voehringer D, Liang HE, Locksley RM. Homeostasis and effector function of lymphopenia-induced “memory-like” T cells in constitutively T cell-depleted mice. *J Immunol.* 2008; 180:4742–4753. [PubMed: 18354198]

32. Henrickson SE, von Andrian UH. Single-cell dynamics of T-cell priming. *Curr Opin Immunol.* 2007; 19:249–258. [PubMed: 17433876]
33. Cyster JG. Chemokines, sphingosine-1-phosphate, and cell migration in secondary lymphoid organs. *Annu Rev Immunol.* 2005; 23:127–159. [PubMed: 15771568]
34. Okada T, et al. Antigen-engaged B cells undergo chemotaxis toward the T zone and form motile conjugates with helper T cells. *PLoS Biol.* 2005; 3:e150. [PubMed: 15857154]
35. Voehringer D, Wu D, Liang HE, Locksley RM. Efficient generation of long-distance conditional alleles using recombineering and a dual selection strategy in replicate plates. *BMC Biotechnol.* 2009; 9:69. [PubMed: 19638212]
36. Sullivan BM, Locksley RM. Basophils: a nonredundant contributor to host immunity. *Immunity.* 2009; 30:12–20. [PubMed: 19144314]
37. Ben-Sasson SZ, Le Gros G, Conrad DH, Finkelman FD, Paul WE. Cross-linking Fc receptors stimulate splenic non-B, non-T cells to secrete interleukin 4 and other lymphokines. *Proc Natl Acad Sci U S A.* 1990; 87:1421–1425. [PubMed: 2106135]
38. Conrad DH, Ben-Sasson SZ, Le Gros G, Finkelman FD, Paul WE. Infection with *Nippostrongylus brasiliensis* or injection of anti-IgD antibodies markedly enhances Fc-receptor-mediated interleukin 4 production by non-B, non-T cells. *J Exp Med.* 1990; 171:1497–1508. [PubMed: 2332730]
39. Le Gros G, et al. IL-3 promotes production of IL-4 by splenic non-B, non-T cells in response to Fc receptor cross-linkage. *J Immunol.* 1990; 145:2500–2506. [PubMed: 2145362]
40. Seder RA, et al. Purified Fc epsilon R+ bone marrow and splenic non-B, non-T cells are highly enriched in the capacity to produce IL-4 in response to immobilized IgE, IgG2a, or ionomycin. *J Immunol.* 1991; 147:903–909. [PubMed: 1830602]
41. Denzel A, et al. Basophils enhance immunological memory responses. *Nat Immunol.* 2008; 9:733–742. [PubMed: 18516038]
42. Obata K, et al. Basophils are essential initiators of a novel type of chronic allergic inflammation. *Blood.* 2007; 110:913–920. [PubMed: 17409268]
43. Ohnmacht C, Voehringer D. Basophil effector function and homeostasis during helminth infection. *Blood.* 2009; 113:2816–2825. [PubMed: 18941115]
44. Kim S, et al. Cutting edge: Basophils are transiently recruited into the draining lymph nodes during helminth infection via IL-3, but infection-induced Th2 immunity can develop without basophil lymph node recruitment or IL-3. *J Immunol.* 2010; 184:1143–1147. [PubMed: 20038645]
45. Gallwitz M, Enoksson M, Hellman L. Expression profile of novel members of the rat mast cell protease (rMCP)-2 and (rMCP)-8 families, and functional analyses of mouse mast cell protease (mMCP)-8. *Immunogenetics.* 2007; 59:391–405. [PubMed: 17342483]
46. Mukai K, et al. Basophils play a critical role in the development of IgE-mediated chronic allergic inflammation independently of T cells and mast cells. *Immunity.* 2005; 23:191–202. [PubMed: 16111637]
47. Finkelman FD, et al. Cytokine regulation of host defense against parasitic gastrointestinal nematodes: lessons from studies with rodent models. *Annu Rev Immunol.* 1997; 15:505–533. [PubMed: 9143698]
48. Finkelman FD, et al. Interleukin-4-and interleukin-13-mediated host protection against intestinal nematode parasites. *Immunol Rev.* 2004; 201:139–155. [PubMed: 15361238]
49. Fallon PG, et al. IL-4 induces characteristic Th2 responses even in the combined absence of IL-5, IL-9, and IL-13. *Immunity.* 2002; 17:7–17. [PubMed: 12150887]
50. Barnden MJ, Allison J, Heath WR, Carbone FR. Defective TCR expression in transgenic mice constructed using cDNA-based alpha-and beta-chain genes under the control of heterologous regulatory elements. *Immunol Cell Biol.* 1998; 76:34–40. [PubMed: 9553774]
51. Veiga-Fernandes H, et al. Tyrosine kinase receptor RET is a key regulator of Peyer's patch organogenesis. *Nature.* 2007; 446:547–551. [PubMed: 17322904]
52. Allen CD, Okada T, Tang HL, Cyster JG. Imaging of germinal center selection events during affinity maturation. *Science.* 2007; 315:528–531. [PubMed: 17185562]
53. Lindquist RL, et al. Visualizing dendritic cell networks in vivo. *Nat Immunol.* 2004; 5:1243–1250. [PubMed: 15543150]

54. Davies SJ, et al. Modulation of blood fluke development in the liver by hepatic CD4+ lymphocytes. *Science*. 2001; 294:1358–1361. [PubMed: 11701932]
55. Delmotte P, Sanderson MJ. Ciliary beat frequency is maintained at a maximal rate in the small airways of mouse lung slices. *Am J Respir Cell Mol Biol*. 2006; 35:110–117. [PubMed: 16484686]

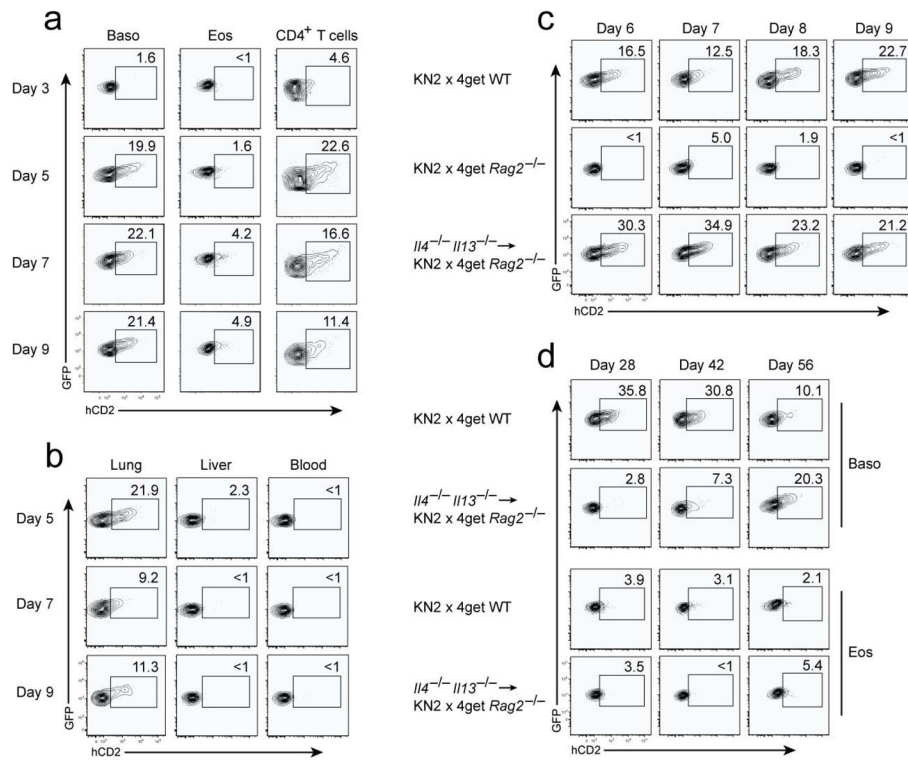


Figure 1. IL-4 production by basophils following parasite infection is restricted to affected tissues

(a) Flow cytometric analysis of IL-4-competent (GFP⁺) cells from the lungs of *N. brasiliensis*-infected KN2 × 4get mice. The gating scheme is presented (Supplementary Fig. 11). Eosinophils and basophils were initially gated as DAPI⁻, GFP⁺ and CD4⁻. Eosinophils are additionally SSC^{hi}, DX5⁻, whereas basophils are DX5⁺, SSC^{lo}. In an effort to normalize the data to all IL-4-competent subsets, only GFP⁺ CD4⁺ T cells are presented. Numbers represent the percent hCD2 minus the percent isotype control for each individual cell population at indicated timepoints. (b) Flow cytometric analysis of hCD2 expression by lung, liver and blood basophils, presented as in (a). (c) IL-4 protein expression, as assessed by membrane hCD2, by lung basophils from KN2 × 4get mice, KN2 × 4get *Rag2*^{-/-} mice, and KN2 × 4get *Rag2*^{-/-} mice reconstituted with *Il4*^{-/-} *Il13*^{-/-} CD4⁺ T cells following *N. brasiliensis* infection. Data are presented as in (a). (d) Flow cytometric analysis of liver basophils and eosinophils from *S. mansoni* infected KN2 × 4get mice and KN2 × 4get *Rag2*^{-/-} mice reconstituted with *Il4*^{-/-} *Il13*^{-/-} CD4⁺ T cells, presented as in (a). Data presented are representative plots from 3–5 independent experiments.

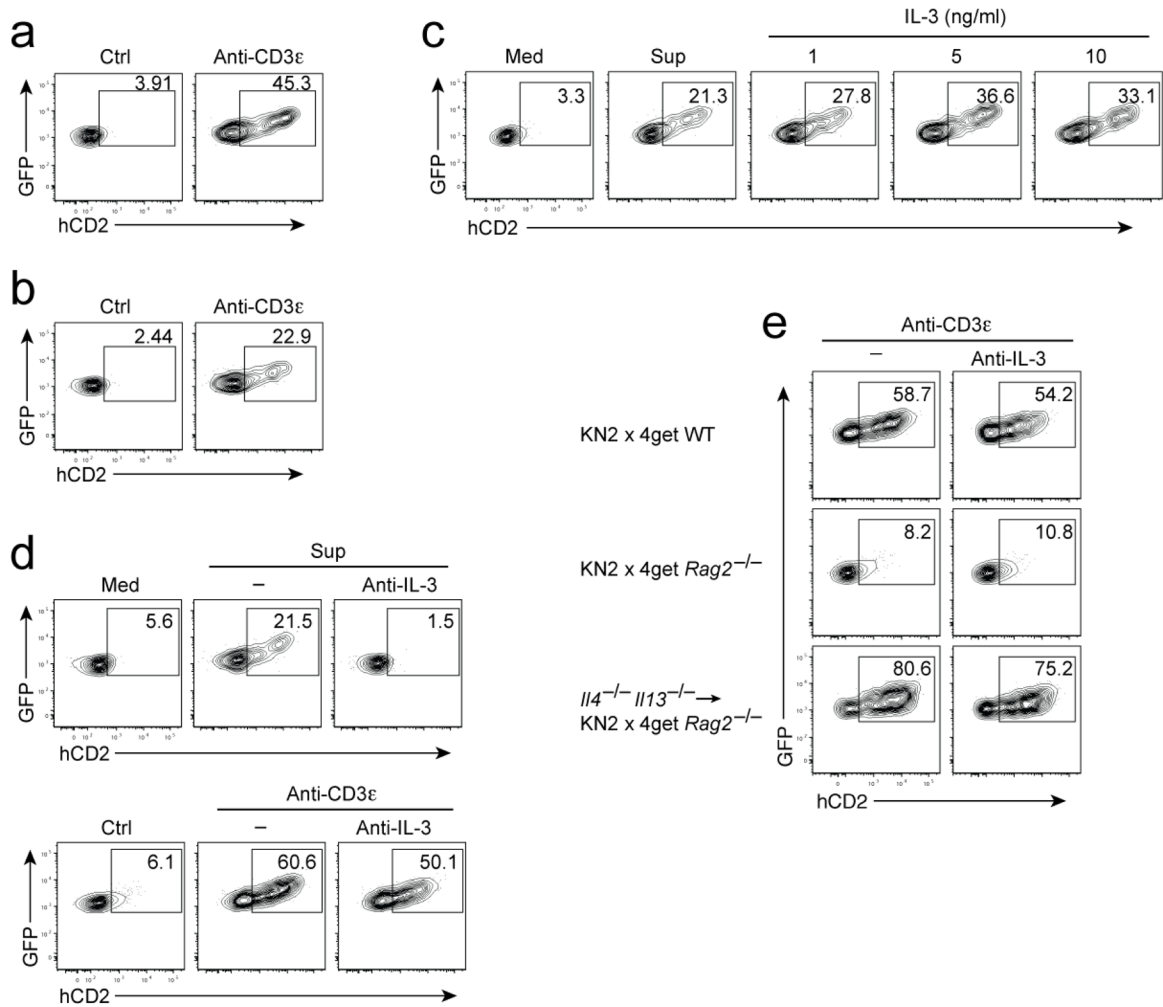


Figure 2. CD4⁺ T cell activation induces basophil IL-4 production *in vitro*

(a) IL-4 expression by basophils following anti-CD3 ϵ stimulation of total splenocytes from *N. brasiliensis*-infected KN2 \times 4get mice. (b) IL-4 expression by basophils enriched from the spleens of KN2 \times 4get *Rag2*^{-/-} mice following anti-CD3 ϵ stimulation of purified CD4⁺ T cells separated by a transwell. (c) IL-4 expression by basophils enriched from the spleens of KN2 \times 4get *Rag2*^{-/-} mice after overnight culturing in activated CD4⁺ T cell supernatant or recombinant IL-3 at the indicated concentrations. (d) Effect of neutralizing anti-IL-3 antibody (10 μ g/ml) on basophil IL-4 production during stimulation of total splenocytes, as in (a), and culturing with activated CD4⁺ T cell supernatant, as in (c). (e) IL-4 expression by basophils enriched from the spleens of *N. brasiliensis* infected KN2 \times 4get, KN2 \times 4get *Rag2*^{-/-} and KN2 \times 4get *Rag2*^{-/-} mice reconstituted with *I14*^{-/-} *I113*^{-/-} CD4⁺ T cells, and stimulated *in vitro* as in (a and d). Data presented are representative of 2–4 independent experiments.

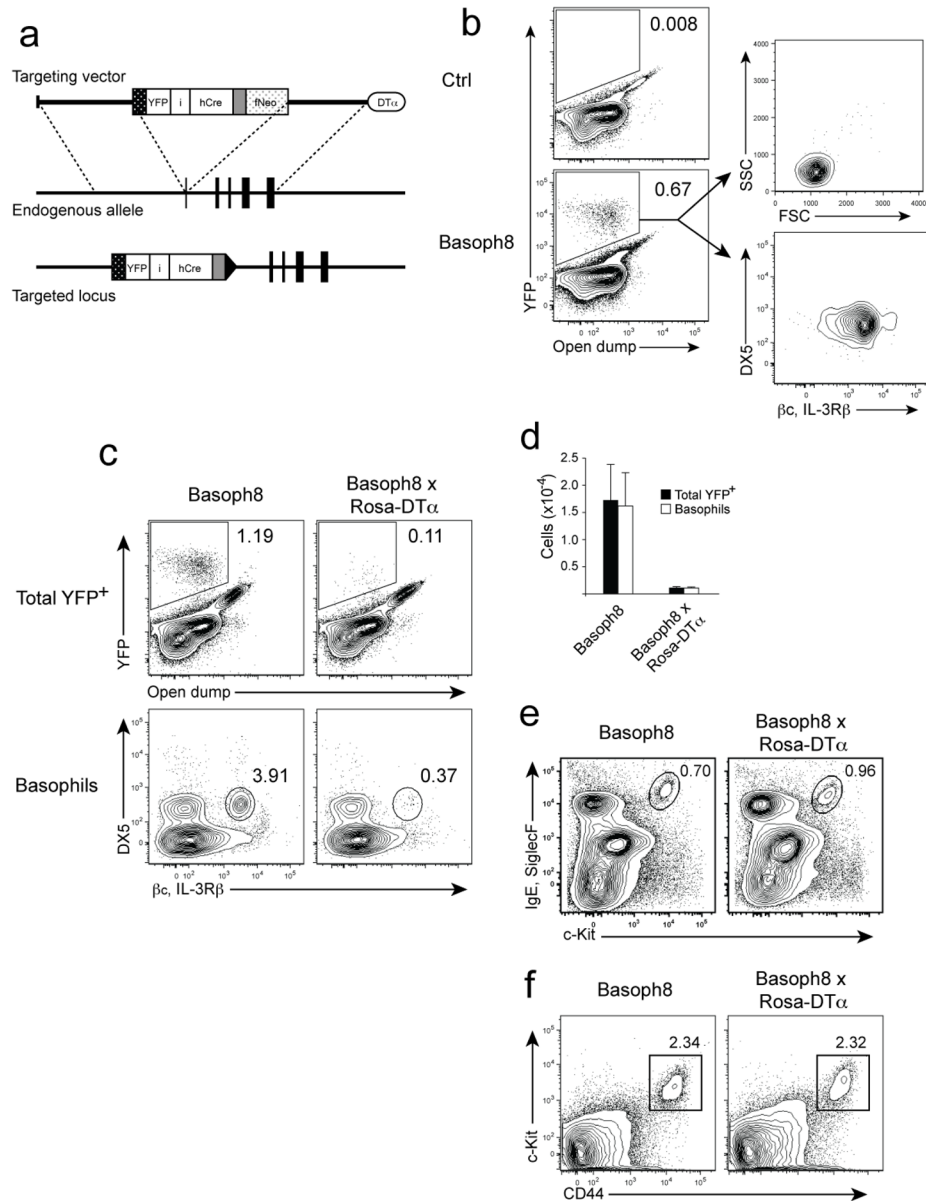


Figure 3. Basophil lineage tracking and deletion in vivo

(a) Schematic illustrating the *mcpt8* targeting strategy used to generate Basoph8 mice. A detailed map and screening of the successful targeting is presented (Supplementary Fig. 4) (b) Flow cytometric analysis of YFP expression in the lung of Basoph8 reporter mice following *N. brasiliensis* infection. Total DAPI⁻, YFP⁺ cells were initially gated based on a non-reporter control. YFP⁺ cells were then assessed for expression of characteristic basophil surface markers. (c) Flow cytometric analysis of basophils in the Basoph8 reporter strain and the basophil deficient Basoph8 \times Rosa-DT α . Total YFP⁺ cells are presented as in (b). Basophils were isolated by conventional flow cytometry by first gating total DAPI⁻, SSC^{lo}, CD4⁻ cells and then subsequent isolation of basophils by their DX5⁺, β c (CD131), IL-3R β ⁺ expression profile. (d) Comparison of basophil numbers versus YFP⁺ cells, isolated as in (c), in both Basoph8 reporter mice and basophil-deficient Basoph8 \times Rosa-DT α mice from the lung following *N. brasiliensis* infection. The graph represents data compiled from 2 independent experiments, 7–8 mice per group. (e) Flow cytometry of peritoneal mast cells

from *N. brasiliensis*-infected mice. (f) Isolation of skin resident mast cell populations in Basoph8 and Basoph8 \times Rosa-DT α mice. Plots are representative of 2–4 independent experiments.

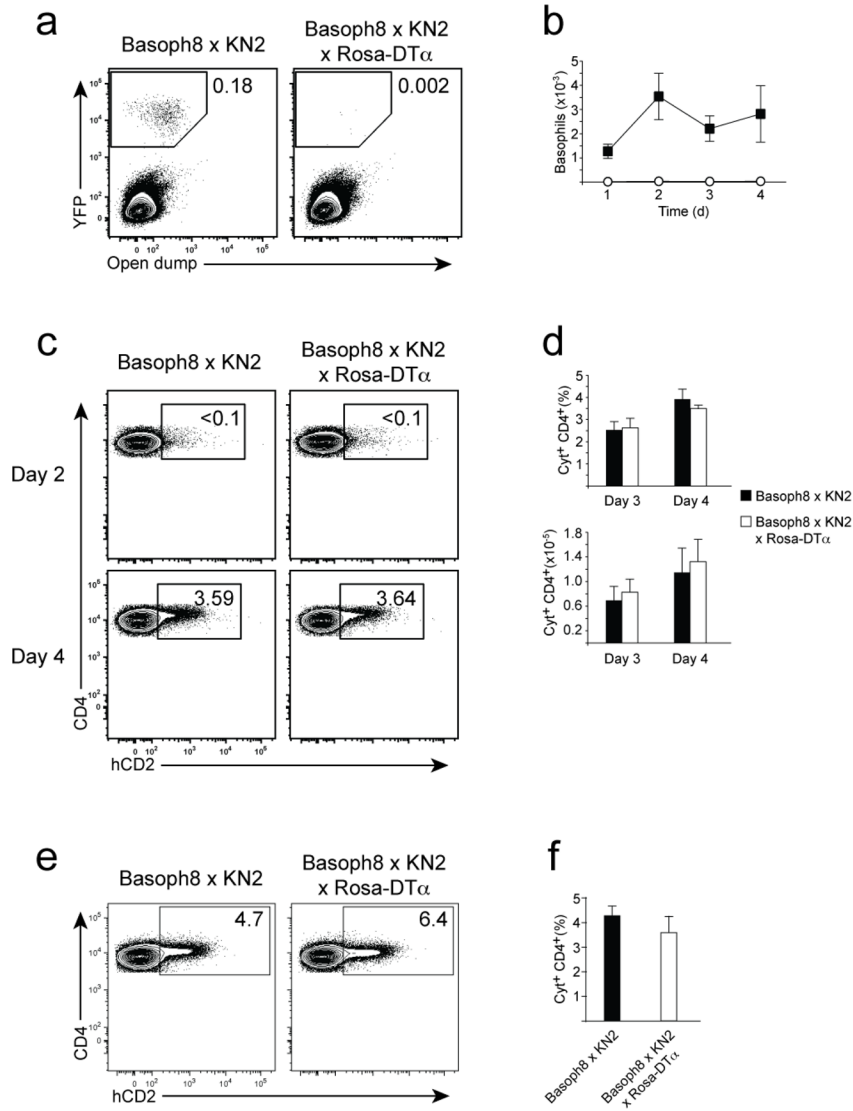


Figure 4. Efficient CD4 $^+$ T cell priming in the absence of basophils

(a) Representative flow cytometric analysis of total YFP $^+$ cells in the draining popliteal node 48 hours after *S. mansoni* egg footpad immunization. Plots represent total live (DAPI $^-$) lymph node cells. (b) Total basophil numbers in the draining node following footpad injection of *S. mansoni* eggs. Data represents the compilation of 3 experiments in which 2–3 mice were analyzed per group, at each timepoint. (c) Flow cytometry of cytokine-positive CD4 $^+$ T cells, as assessed by hCD2 surface expression, in the draining node 4 days after *S. mansoni* egg immunization. Plots represent total CD4 $^+$, DAPI $^-$ cells, and hCD2 staining was analyzed as in (Supplementary Fig. 11) (d). The graphs represent the percent of hCD2 $^+$, cytokine-producing CD4 $^+$ T cells (top) and the total number of cytokine positive CD4 $^+$ T cells (bottom) on days 3 and 4. Data was compiled from 3 independent experiments as in (b) and is presented as the mean \pm SEM. (e) Representative flow cytometric analysis of hCD2 $^+$ CD4 $^+$ T cells, as in (c), 72 h following papain (50 μ g) footpad immunization. (f) Percent cytokine positive CD4 $^+$ T cells compiled from 3 independent experiments with 2–3 mice per group presented as the mean \pm SEM.

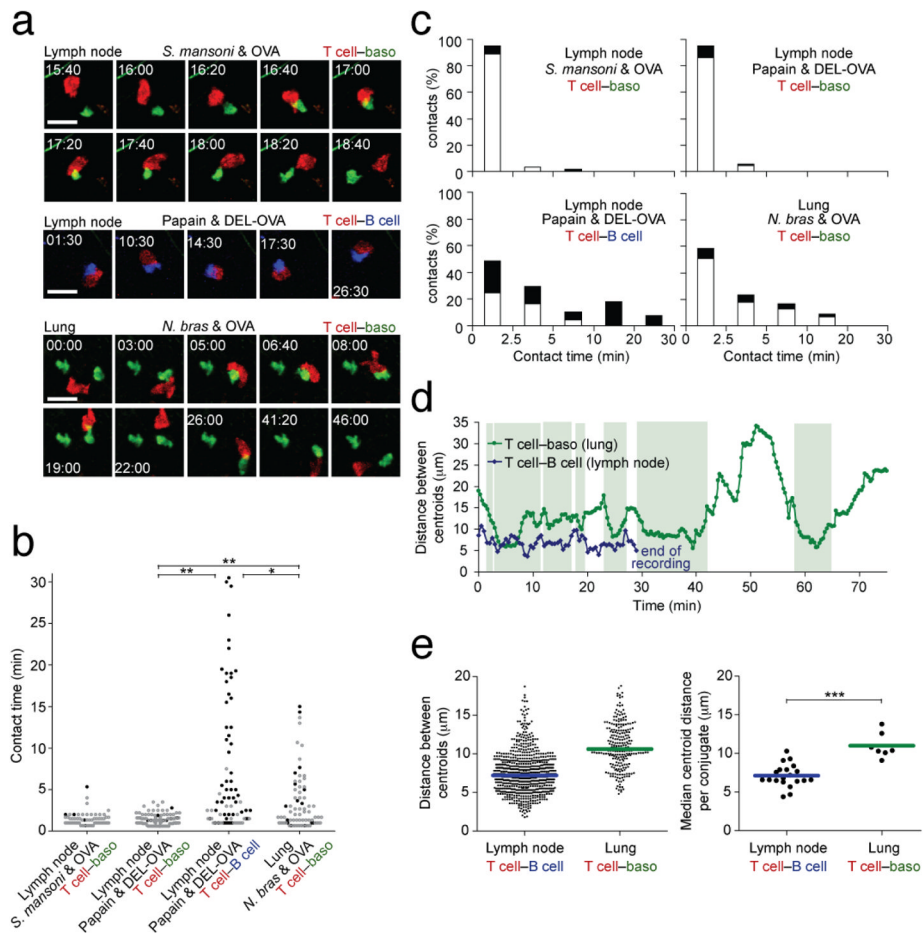


Figure 5. Basophils and CD4⁺ T cells interact in the lungs but not in lymph nodes

(a) Representative time-lapse images of contacts between the indicated cell types. Images are maximum intensity z-projections (upper, middle, and lower are 33 μm , 30 μm and 28 μm projections, respectively) from cropped two-photon microscopy image stacks. The contacts in the middle and lower panels are further characterized in (d) and Supplementary Fig. 8). The lower panels (lung) correspond to Supplementary Video 4. Elapsed time is shown as min:sec. Scale bars, 20 μm . (b) Duration of contacts observed between the indicated cell types. Each dot represents the duration of a single contact. Grey circles indicate contacts that could be completely observed from start to finish, whereas black dots represent contacts that could not be tracked for their entire duration, typically because the conjugate entered or exited the imaging volume or exceeded the duration of the recording. The black dot measurements therefore are underestimates. *, $P < 0.05$; **, $P < 0.01$ (Kruskal-Wallis test). (c) Histograms compiling the data in b. Black bar segments indicate conjugates that could not be tracked for their entire duration. (d) Measurements of the distance between cell centroids for the cell contacts shown in a. The T cell and basophil were only in contact during the time periods that are shaded in light green. In contrast, the T cell-B cell conjugate shown persisted for the entire duration of a 30-minute timelapse recording. (e) On the left panel, dots represent single timepoint measurements of the distance between cell centroids for cells that remained in contact for longer than eight minutes. Measurements are only shown for the timepoints in which the cells were directly in contact with each other. These data are compiled on the right panel, showing the median

centroid distance for each cell conjugate that lasted greater than eight minutes. *, $P = 0.0003$ (Mann-Whitney U-test).

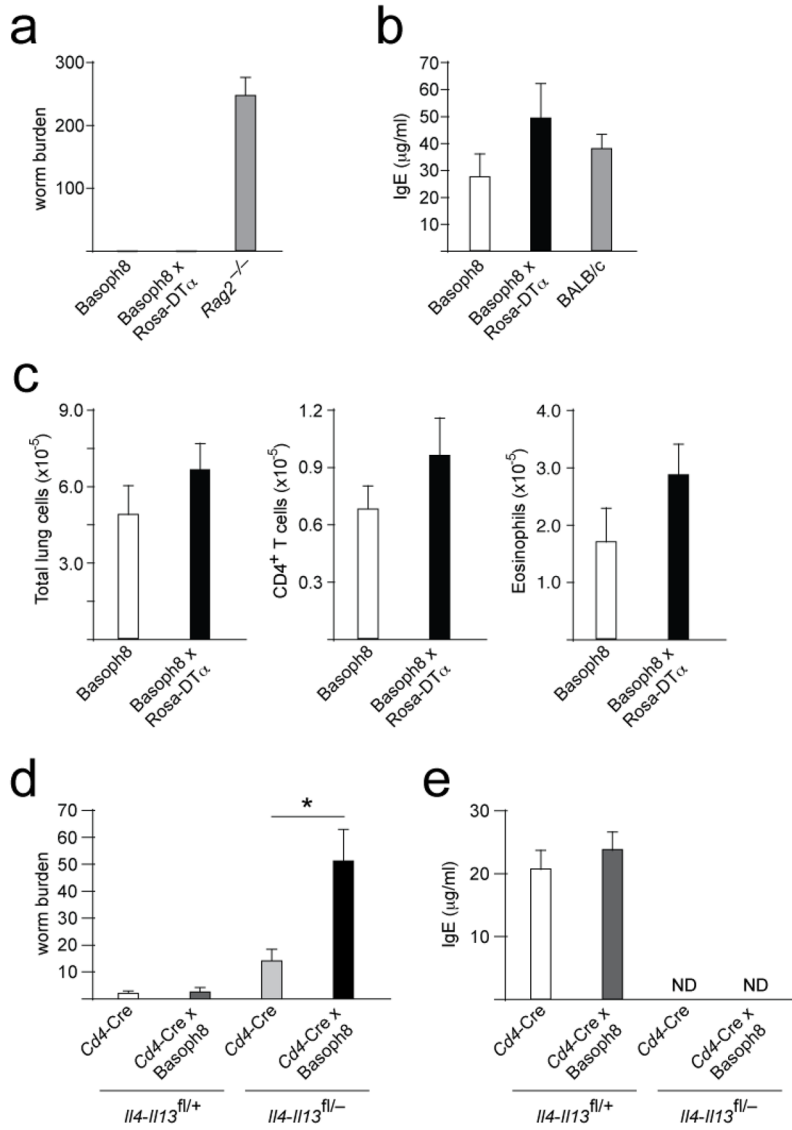


Figure 6. Basophil derived cytokines contribute to anti-helminth immunity

(a) Worm burden in the small intestine 10 days following primary *N. brasiliensis* infection. Data was compiled from 3 independent experiments in which 3–5 mice per group were infected. (b) Serum IgE concentrations of cohorts in (a) and BALB/c control mice. (c) Analysis of the inflammatory response in the lung of experiments presented in (a). Cellularity was determined by flow cytometric analysis. (d) Worm burden in the small intestine as in (a). Data represents the compilation of 2 experiments and a total of 5–8 mice per group. *, $P = 0.0036$ (e) Serum IgE concentrations from the cohorts presented in (d). Data in each panel is presented as the mean \pm SEM.